Sparse Representations on DW-MRI: A study on pancreas

Anastasia Pentari[1,2], Grigorios Tsagkatakis[2], Kostas Marias[2,3], Georgios C. Manikis[2], Nikolaos Kartalis[4], Nikolaos Papanikolaou[5], Panagiotis Tsakalides[1,2].

[1]Department of Computer Science, University of Crete.
[2]Institute of Computer Science, Foundation of Research and Technology – Hellas (FORTH), Heraklion, Greece.
[3]Department of Electrical and Computer Engineering, Hellenic Mediterranean University, Greece.
[4]Department of Radiology, Karolinska University Hospital, Stockholm, Sweden.
[5]Clinical Computational Imaging Group, Centre for the Unknown, Champalimaud Foundation, Lisbon, Portugal.

Abstract—This paper presents a method for reducing the Diffusion Weighted Magnetic Resonance Imaging (DW-MRI) examination time based on the mathematical framework of sparse representations. The aim is to undersample the b-values used for DW-MRI image acquisition which reflect the strength and timing of the gradients used to generate the DW-MRI images since their number defines the examination time. To test our method we investigate whether the undersampled DW-MRI data preserve the same accuracy in terms of extracted imaging biomarkers. The main procedure is based on the use of the k-Singular Value Decomposition (k-SVD) and the Orthogonal Matching Pursuit (OMP) algorithms, which are appropriate for the sparse representations computation. The presented results confirm the hypothesis of our study as the imaging biomarkers extracted from the sparsely reconstructed data have statistically close values to those extracted from the original data. Moreover, our method achieves a low reconstruction error and an image quality close to the original.

Keywords—Sparse Coding, Dictionary Learning, DW-MRI, b-value, IVIM.

I. INTRODUCTION

Magnetic Resonance Imaging (MRI) is a medical imaging technique used widely in radiology in order to acquire anatomical and functional images to assess pathophysiology. MRI involves different techniques and imaging protocols depending on the organ/ pathology imaging. A well-known such technique is the Diffusion-Weighted Imaging (DWI) which provides significant information about tissue cellularity and microstructure. DWI most characteristic index is the so-called *b-value*, a parameter which controls the sensitivity of DWI contrast to the water mobility. Although this technique has been used since mid-1980'for characterizing pathophysiology in an efficient and non-invasive way, the long examination time remains an issue in many clinical imaging applications.

DWI aims to generate diffusion weighting in an image, i.e. a restricted diffusion sensitivity, which is based on the choice of the applied b-value. Specifically, in healthy areas, water molecules are not stationary while in pathological conditions, such as in tumours, this motion is restricted by the presence of many abnormal cells (hypercellularity). As a result, molecules signal intensity (basically of voxel of interest-VOI) is measured and thus it is considered necessary to apply both low (0-50 s/mm^2) and high (up to 800 s/mm^2) b-values, so as to acquire slices with multiple contrasts in order to achieve better evaluation of malignancy indication [1]. To this end, this procedure helps clinicians to extract significant biomarkers from representative motion models, such as the Intravoxel Incoherent Motion (IVIM) model. These biomarkers can be interpreted appropriately by clinicians, giving though extra information about the examined disease. A thorough review can be found in [2].

In the past many researchers have focused on the solution of reducing the MRI examination time problem. Compressive Sensing techniques have widely used on MRI, by basically undersampling the k-space [3]. Other studies, which are based on CS methods, provide a principled approach to undersample the number of acquired slices or the number of the pixels from each slice. On the other hand, our spatial-domain-based method tries to reduce the DWI data acquisition time in terms of b-values via sparse representations. Our working hypothesis is to sample 3 (out of 8) b-values but provide the whole examination to the clinicians, in the end, by synthetically computing the missing ones. Moreover, the proposed methodology not only undersamples the number of the b-values but also the number of the pixels/patches of the available data in each b-value image acquisition. Finally, an IVIM model's biomarkers analysis is applied to ensure that there aren't any accuracy compromises in the biomarkers extracted from the sparse data.

The rationale behind this work lies on the fact that a Sparse Representation technique could probably reduce the necessary b-values for the extraction of clinically significant biomarkers. This in turn means that the long examination time could be reduced, alleviating patient discomfort and allowing more examinations within the hospital working hours leading to a positive socioeconomic effect in the healthcare system. A first challenge therefore is to reduce the number of the acquired data from 8 (according to the pancreas examinations) to 3 b-values, two low and one high. After that, the most significant results evaluation concerns the IVIM biomarkers statistical analysis, i.e. the original and the synthetic to be as close as possible, and finally to achieve a reconstructed image quality not far from the original.

II. MATERIAL AND METHODS

The sparse representations framework has become a powerful tool with valuable results in many fields such as machine learning and signal-image processing [4,5,6]. This technique belongs to the Compressed Sensing (CS) family. It is based on two steps, the sparse coding and the dictionary learning. Sparse Representation method's basic procedure is to employ a few feature/atoms from a learned dictionary and

with the use of a sparse coefficient manage to approximately reconstruct the whole original data/examination based on the use of only 3 out 8 b-values. There exists a variety of suitable algorithms for the Sparse Representation method, although in this work was used a combination of two simple, efficient and fast algorithms, the OMP and the k-SVD for the computation of the sparse coefficient and the learning of the dictionary procedure, respectively. In the next subsection the proposed methodology is described.

The problem that we tried to solve is presented in equation (1). It is important to understand that the sparse representation problem is based on two interrelated steps, the computation of the dictionary A and the computation of the sparse representation X.

$$\min\{\|Y - AX\|_F^2\}$$
$$subject\ to: \|x_i\|_0 \leq T_0, \forall i \qquad (1)$$

In equation (1), $Y \in R^{72 \times 1}$ denotes the original data of patch size 3×3 (and for 8 b-values), $A \in R^{72 \times K}$ is the training dictionary of number of atoms/columns K and $X \in R^{K \times 1}$ the sparse coefficient vector. The zero-norm counts the non-zero elements of x while T_0 denotes the sparsity level. In the above problem, we minimize the reconstruction error between the original patch-images and the reconstructed (AX), computed by using our method. As mentioned, the two basic steps are the sparse coding level and the dictionary update stage. Each one of them worked alone, i.e. it was kept fixed in order to take two convex optimization problems (as alone is a non-convex one). Finally, F is the Frobenius norm.

A.   Sparse Coding

Matching Pursuit (MP) is an iterative greedy algorithm which finds the sparse representation of a signal-image. At each iteration, MP algorithm aims to find the atoms which have the highest correlation with the approximation error. The final sparse solution is given by combining the selected atoms with a weight corresponding to their correlated values. In this study the OMP algorithm is used, a fast and precise method. The only difference with the MP is that OMP updates the coefficients of all previously selected atoms per iteration. Through this method, x is computed (a vector with a lot of zero elements).

B.   Dictionary Update

Suitable for this stage was the k-SVD algorithm. This algorithm is simple, fast and flexible. It does not work alone but in conjunction with any Matching Pursuit (MP) algorithm. Its main procedure is the k_{th} column/atom update of the dictionary each time. The dictionary is trained through samples, i.e. patches of the available images-data. The algorithm's goal is to converge in 100 iterations, i.e. the reconstructed data should be as close to the original as possible. Through this method, A is computed (a matrix that based on x sparse gives the reconstructed results). Note that the atoms/columns of a dictionary have to be normalized (norm equal to one). Moreover, A has to be overcomplete, i.e. the number of atoms has to be much larger than its rows.

At this level of our analysis, imagine that a dictionary has trained.

C.   Reconstruction

At this point, a dictionary has been trained. At last, the final procedure is the examination reconstruction. As we aimed to reduce the number of the acquired b-values, the dictionary used was of smaller size than the trained one. To be more specific, imagine that clinicians acquire 3 out of 8 b-values needed for pancreas. A dictionary of size $27 \times K$ is available. Then by the already trained dictionary of size $72 \times K$ the whole examination, through a procedure that will be analysed, is computed.

At the experimental procedure, all possible 3 b-value combinations were checked. Practically, by finding the best 3 b-value combination, specific rows of the trained dictionary were selected. Note that, the best combination was the one with the smallest reconstruction error. A significant observation was the following: through the experiments, we noticed that the norm of the initial column-dictionary divided by the norm of the reduced column-dictionary was greater than one. This happened because the number of rows in the "reduced dictionary" was smaller than the trained, and this was indeed our goal. The division of these two norms gave a normalization coefficient necessary for the accurate image reconstruction. This fact is necessary as by condition the dictionaries have to be normalized. So, for one patch the basic procedure is the one described in the next equations (2-5).

$$X^{K \times 1} = OMP(A^{27 \times K}) \qquad (2)$$
$$\forall i = 1, \cdots, K: x_{new}(i) = c \cdot x(i) \qquad (3)$$
$$c = \|A^{72}(i_{th})\| / \|A^{27}(i_{th})\| \qquad (4)$$
$$Y^{72 \times 1} = A^{72 \times K} \cdot X_{new}^{K \times 1} \qquad (5)$$

A is the dictionary, 72 denotes the dictionary size for all the b-values while 27 is the dictionary size for 3 b-values. X denotes the sparse coefficient and c is the normalization coefficient computed by the division mentioned. Finally, i_{th} is one out of the K dictionary's columns. In the next section a brief description of the experimental conditions optimizations are presented.

D.   Problem Optimizations

By "problem optimization" we denote steps that helped us take more accurate results. Analytically, DW-MRI images have many specific features. First of all each examination has anatomical correspondence, i.e. each body slice has a continuity from the previous and the next slices and it is not randomly placed in this sequence. Through our experiments it was observed that, in order to "exploit" this correspondence, it was necessary to use one dictionary per slice. This fact gave a lower reconstruction error between the original and the synthetic-data intensities. Moreover, MRI images contain a lot of background information which was confusing since it added non-useful signal intensity patches to the possible solutions. As a remedy, we restricted the Region of Interest (ROI) to a smaller one, which contained the pancreas (i.e. the pathology) and a part of the rest of the image, with healthy tissues, at the training stage. It was observed that this optimization gave more accurate results (i.e. lower reconstruction error).

III. IVIM

The so called b-value depends on the diffusion gradients. Two b-value acquisitions give better precision. However, more than two b-values give better accuracy and additional information on tissue microstructure. That is why we use the IVIM model in our study. The IVIM model is a more complicated model than the simple mono-exponential (ADC) model. It gives information about both diffusion and perfusion. The study of the combination of the diffusion and the blood microcirculation are two completely separate phenomena. Specifically, the IVIM model extracts diffusion and perfusion information in each voxel, information which gives further detail for the pathology, in comparison to the ADC model, which extracts only diffusion information. It can be described as a bi-exponential equation, shown in (6).

$$\frac{S}{S_0} = f e^{(-bD^*)} + (1-f)e^{(-bD)} \qquad (6)$$

where $\frac{S}{S_0}$ is the overall MRI signal attenuation, f is the flowing blood fraction, D is the water diffusion coefficient and D^* is the pseudo-diffusion parameter. Comparing the mono-exponential and the bi-exponential models, IVIM gives more accurate results regarding the true motion than the ADC. It is a very sensitive model, especially in low b-values ($< 200 \ s/mm^2$). This sensitivity is more apparent in the D^* computation and this was in line with our results too, since by avoiding specific low b-values, the D^* parameter exhibited non-comparable values, compared to the other two biomarkers [8].

IV. STATISTICAL ANALYSIS

The criteria chosen for a robust statistical analysis of the proposed results concerned the following facts: First of all, the most significant and general comparison was the statistical analysis among three experimental cases, the original, the sparse reconstruction and the linear interpolated, based on 3 retained b-values. The reason for choosing the simple linear interpolation was to facilitate the comparison between the measurements of our method and the sparse, 3 b-values case.

More specifically, a clinically important question concerned the extraction of the three IVIM model biomarkers (D, D^*, f) and the comparison of the mean and standard deviation from the original and reconstructed data. Specifically, the set of these statistical biomarkers was extracted from each of the 12 patients analyzed. First, the pathology regions of interest (ROIs) were isolated and then each biomarker was computed in each ROI pixel. Finally, the mean and standard deviation of each biomarker in the ROI was computed.

In order to assess the reconstruction error, the Normalized Root Mean Square Error (NRMSE) was computed. This reconstruction error computes the signal intensities (SIs) differences between the original and the examined (reconstructed) case. A low NRMSE indicates that the SIs are close enough. Moreover, it was our algorithmic stopping criterion, for appropriate values of atoms, sparsity level and training samples, i.e. the smallest NRMSE between the experimental tries, showed the algorithmic parameters that we had to use.

Last but not least, the Signal-to-Noise-Ratio (SNR) concerning the MRI images processing, was also reported. The SNR of the MRI images were computed by first using the tumor ROI and then by selecting a ROI at the background (called air), followed by the SNR computation from equation (7).

$$SNR = \frac{SI_{tumor}}{\sqrt{\frac{2}{4-\pi}} sd_{air}} \qquad (7)$$

where, SI_{tumor} refers to the pixel intensities of the tumor area and sd_{air} the standard deviation of an area selected on the background, not including any tissue [1].

V. RESULTS

This section describes the most important results of our procedure. The experimental characteristics were the following: the available anonymous patients were 12. Each examination led to a 4D matrix of size ($148 \times 180 \times 40 \times 8$), i.e. 40 slices of 8 b-values and each slice size was (148×180) pixels. In order to train a dictionary for each slice-anatomical position, the suitable number of atoms was 400, the number of training randomly chosen samples/patches was 3500, and finally the sparsity level which gave the best results was 5, i.e. the number of the maximum atoms to be used at the sparse coding procedure.

According to the dictionary size, for all the b-values it was (72×400), i.e. ((($3 \times 3) \times 8) \times 400$), where ($3 \times 3$) was the patch size. Through the leave-one-out method all patients were tested, which means that one patient was kept for testing and the rest of them for training. As mentioned, a part of the image was used for training, chosen near the pathology including the pancreas. Each slice of size ($148 \times 180 \times 8$) was split into overlapping patches, of 1 pixel overlap. At the training stage, having 11 patients chosen, and for each selected slice out of the 40, the selected ROIs from all the patients were stored in a matrix, which was shuffled (per row, as the column corresponded to the b-values), and then patches were randomly chosen in order to help the training of the dictionary.

Before reporting the results, it is reminded that, the experimental cases compared, were the original, the sparse and the linear interpolated, based on 3 b-values (the two last). These 3 b-values were not randomly selected; the b0 and the b1000 were always retained, while the third one was selected through extensive experimentation, and found to be b100 which yielded the smaller reconstruction error and the best biomarkers. As a result, by 3 b-values we refer to the b-value combination of 0-100-1000. The first and the last b-values were always kept fixed since they provide significant clinical information. Finally, the IVIM biomarkers (D, D^*, f) were computed through the DMT tool [9] for each patient and were extracted from the pathology ROI area only.

In table I, we report the most significant results of our analysis including not only the IVIM model's mean value biomarkers, which also indicate that the SIs of the original pathology area and the sparse reconstructed are very close in intensity, but also the variance. Specifically, observing the equation (6), it is noticeable that the biomarkers are closely connected with the SIs of the images. As a result, a major

goal was to reconstruct slices/examinations with a small reconstruction error. Table I presents a per-patient analysis of the mean and standard deviation of the IVIM biomarkers in the original, spare and interpolated datasets. It is apparent that in the original and the sparse cases, of the mentioned b-value combination, the extracted biomarkers were very close (Interclass Correlation Coefficient-ICC 80% and 87% for D and f, respectively), i.e. in acceptable margins, as we can infer from the mean and standard deviation values. It is worth mentioning that in the case of keeping all the b-values and evaluating the sparse-procedure performance the correlations were 84.9% and 93.6% for D and f, respectively. On the other hand, it is important to comment the linear interpolated case performance. The linear interpolation was the simplest choice for comparison with our method, and as it figured out from table I, the calculated interpolated-biomarkers are not so close (with very low correlations) as the sparse-biomarkers, which indicates that the sparse representation procedure can provide more clinically suitable results, in a linear way.

The region of interest, as mentioned, was chosen to be the pathology of the pancreas. We chose to evaluate our method on tumor tissue since this is the most important challenge in the sense that tumor tissue exhibits heterogeneity and it is important to preserve it for diagnostic purposes, after reconstruction. We also plan a more extensive study validating our method on both healthy and tumorous areas and compare performance also in terms of tissue type.

These areas were stored in a pixel-level-matrix and the mean value of the whole pathology was computed (as well as the corresponding biomarkers). Note that the NRMSE was of order 10^{-6}, between 0 and 1 (normalized) showing that the fitting performance was good enough and in any case also smaller than the interpolated case.

In figure 1b, a comparison of the SNR between the original, the sparse, the interpolated and a noisy random case were held. It observed that, the original case has a lower quality compared to the sparse one, which can be attributed to the fact that the sparse representation procedure can also be used for denoising [10]. Also, the interpolated case exhibited a lower quality result, very noisy, compared to the noisy experimental case. Note that in the noisy case (green line), Rician noise was added in the original images in order to have a better comparison measurement and to prove how noisy the interpolated images were. The main quality differences appeared, mostly, in the higher b-values.
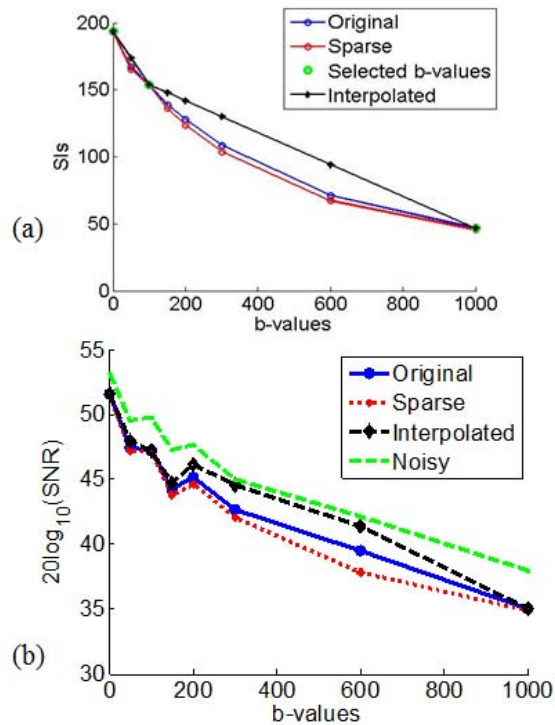
	mean value								
	original			interpolated			sparse		
patient	D	D*	f	D	D*	f	D	D*	f
1	1.33	50.35	0.14	1.15	54.07	0.09	1.36	50.59	0.16
2	1.13	61.19	0.11	1.01	59.77	0.08	1.16	33.20	0.13
3	1.18	72.58	0.19	1.02	31.58	0.17	1.18	133.24	0.23
4	1.12	46.94	0.20	0.99	40.36	0.17	1.13	38.09	0.22
5	1.09	80.52	0.12	0.95	52.97	0.11	1.09	73.01	0.15
6	1.25	53.59	0.15	1.10	52.14	0.11	1.26	80.50	0.18
7	1.03	91.78	0.15	0.93	41.65	0.12	1.04	46.31	0.17
8	1.31	61.28	0.12	1.13	61.01	0.11	1.34	78.13	0.19
9	1.32	55.86	0.15	1.10	66.97	0.10	1.28	25.67	0.16
10	1.24	67.41	0.13	1.05	57.37	0.09	1.22	78.69	0.13
11	1.27	90.24	0.15	1.13	66.52	0.12	1.30	36.35	0.21
12	1.16	53.10	0.10	1.05	67.57	0.07	1.22	133.12	0.12
	standard deviation								
1	0.24	91.85	0.12	0.17	74.48	0.10	0.18	97.06	0.12
2	0.21	104.51	0.10	0.18	82.37	0.09	0.18	72.82	0.11
3	0.23	104.71	0.10	0.16	32.50	0.11	0.12	136.97	0.08
4	0.21	82.44	0.12	0.20	62.20	0.15	0.18	72.48	0.13
5	0.21	117.48	0.12	0.17	80.45	0.13	0.17	115.05	0.13
6	0.25	94.32	0.11	0.18	73.82	0.09	0.20	120.00	0.10
7	0.22	120.76	0.11	0.18	58.64	0.12	0.17	87.00	0.11
8	0.30	98.89	0.10	0.20	81.01	0.10	0.24	119.87	0.11
9	0.31	99.21	0.14	0.23	91.65	0.13	0.27	56.22	0.13
10	0.37	109.75	0.11	0.27	81.32	0.09	0.36	118.88	0.11
11	0.20	121.16	0.12	0.15	84.25	0.13	0.18	76.15	0.12
12	0.22	94.79	0.09	0.17	92.63	0.09	0.16	141.53	0.09

Table I: Per patient analysis of mean and standard deviation of the biomarkers of the IVIM mode.

In figure 1a, it is observed how close were the initial/original SIs in comparison to the sparse ones. On the other hand the interpolated were far from the original.

Fig.1: (a) Comparison of original, sparse and interpolated data on signal intensity level. (b) Comparison of SNR between experimental cases.

To be more specific, in figure 2, an optical image example is presented, showing that in the case of the 5th (200 s/mm^2) b-value the sparse result is smoother than the original and the interpolated. This happens due to the fact that patch –level analysis was held, meaning that, at the reconstruction stage a mean value of the overlapping patches was implemented.

On the other hand, in figure 3, the 7th b-value, i.e. 600 s/mm^2 of the first patient also presented, showing an important visual difference between the sparse reconstruction and the original data. The 7th b-value was chosen because as shown in figure 1b, it exhibits large SNR deviations. Note that that 7th b-value is also a reconstructed one from our 3-b-

value method, as the 6th. The sparse reconstruction not only gave a much smoother result but also a less grainy (i.e. spotted) appearance. This phenomenon is mostly observed in areas near the background, far from the tumorous pixels.

Finally, it is important to comment on the biomarker D^*. The pseudo-diffusion parameter is very sensitive, especially in low b-values, and this was also apparent throughout our procedure, leading to inconsistent results.

Fig.2: Comparison of the original, sparse and interpolated cases of the 5th b-value of a patient.

Fig.3: Comparison of the original, sparse and interpolated case of the 7th b-value of the same patient.

VI.   DISCUSSION

Diffusion imaging is undoubtedly a very important method for detecting malignant tissues in various anatomical areas. Diffusion model performance in terms of its fitting quality and selection of the most statistically relevant model for characterizing malignant areas in several anatomical sites are issues of crucial importance [1]. The present study focused on reducing the acquisition time required to well-preserve the values of imaging biomarkers from the IVIM diffusion model. The main goal of this work was to confirm the feasibility of extracting IVIM biomarkers from the sparse data with values close to the ground truth (i.e. IVIM biomarkers extracted from the original data).

The presented results based on the reconstructed images and especially the pathology areas indicate that the presented method can reduce the number of b-values during image acquisition without compromising the accuracy of the IVIM imaging biomarkers. Secondly, proposed method was found to perform better than the interpolation one based on several criteria, such as the $NRMSE$, and the SNR. Finally, the reconstruction was performed with a small reconstruction error. Our experiments showed that by keeping only 3 (out of 8) b-values and reconstructing the rest of them, the quantitative biomarker results can be computed with acceptable accuracy for the assessment of pancreatic DWI-MRI images. It is important to note that keeping 3 b-values is the minimum number possible for the IVIM model especially since the D^* parameter is affected.

VII.   CONCLUSIONS

In this study, we demonstrated initial feasibility for reducing the DW-MRI image acquisition time by reducing the b-values and demonstrating that the extracted biomarkers from the sparse data were close to the ground truth. While our results are very encouraging there is still a lot of work needed to improve our method (e.g. find a more effective method of computing the sensitive pseudo-diffusion parameter), and demonstrate overall efficiency and robustness. Nevertheless, our results confirm that sparse representations are valuable towards reducing MRI examination time for alleviating patient discomfort and optimizing the use of hospital scanner resources.

REFERENCES

[1]   Manikis GC, Marias K, Lambregts DMJ, Nikiforaki K, van Heeswijk MM, Bakers FCH, Beets-tan RGH, Papanikolaou N., Diffusion weighted imaging in patients with rectal cancer: Comparison between Gaussian and non-Gaussian models. PloS one. 2017, 12(9):e0184197.

[2]   Manikis GC, Kontopodis E, Nikiforaki K, Marias K, Papanikolaou N. Imaging Biomarker Model-Based Analysis, Imaging Biomarkers: Springer; 2017. p. 71-86.

[3]   Michael Lustig, David Donoho, and John M. Pauly, Sparse MRI: The application of Compressed Sensing for rapid MRI imaging, Magnetic Resonance in Medicine 2007, 58: p. 1182-1195.

[4]   E. Troullinou, G. Tsagkatakis, G. Palagina, M. Papadopouli, S. Smirnakis, and P. Tsakalides, Dictionary Learning for Spontaneous Neural Activity Modeling, in Proc. 25th European Signal Processing Conference(EUSIPCO 17), Kos island, Greece, August 28 September 2, 2017.

[5]   K. Fotiadou, G. Tsagkatakis, and P. Tsakalides, Spectral Resolution Enhancement of Hyperspectral Images via Sparse Representations, in Proc. 2016 IS&T International Symposium on Electronic Imaging, Computational Imaging, San Francisco, CA, February 15-19, 2016.

[6]   K. Fotiadou, G. Tsagkatakis, and P. Tsakalides, Low Light Image Enhancement via Sparse Representations, in Proc. International Conference on Image Analysis and Recognition (ICIAR 14), Vilamoura, Algarve, Portugal, October 22-24, 2014.

[7]   Chilla GS, Tan CH, Xu C, Poh CL. Diffusion weighted magnetic resonance imaging and its recent trend-a survey. Quant Imaging Med Surg. 2015;5(3):407-22.

[8]   -Dow-Mu Koh, David J. Collins, Matthew R. Orton, Intravoxel Incoherent Motion in Body Diffusion-Weighted MRI: Reality and Challenges, Medical Physics and Informatics, June 2011.

[9]   Manikis GC, Nikiforaki K, Papanikolaou N, Marias K., Diffusion Modelling Tool (DMT) for the analysis of Diffusion Weighted Imaging (DWI) Magnetic Resonance Imaging (MRI) data. Proceedings of the 33rd Computer Graphics International; Heraklion, Greece: ACM; 2016.

[10] Vishal Patel, Yonggang Shi, Paul M. Thompson, Arthur W. Toga, K-SVD FOR HARDI DENOISING, Laboratory of NeuroImaging, University of California, Los Angeles, IEEE, 2011.